The official journal of the Japan Atherosclerosis Society and
the Asian Pacific Society of Atherosclerosis and Vascular Diseases

Original Article

J Atheroscler Thromb, 2019; 26: 915-930. http://doi.org/10.5551/jat.48405

Rivaroxaban Suppresses the Progression of Ischemic Cardiomyopathy in a Murine Model of Diet-Induced Myocardial Infarction

Jingyi Liu[1], Makoto Nishida[1, 2], Hiroyasu Inui[1], Jiuyang Chang[1], Yinghong Zhu[1], Kotaro Kanno[1], Hibiki Matsuda[1], Masami Sairyo[3], Takeshi Okada[1], Hajime Nakaoka[4], Tohru Ohama[1, 5], Daisaku Masuda[6], Masahiro Koseki[1], Shizuya Yamashita[1, 6, 7] and Yasushi Sakata[1]

[1]Department of Cardiovascular Medicine, Osaka University Graduate School of Medicine, Suita, Osaka, Japan
[2]Health and Counseling Center, Osaka University, Toyonaka, Osaka, Japan
[3]Department of Cardiology, Kawanishi City Hospital, Kawanishi, Hyogo, Japan
[4]Department of Cardiology, Kakogawa Central City Hospital, Kakogawa, Hyogo, Japan
[5]Department of Dental Anesthesiology, Osaka University Graduate School of Dentistry, Suita, Osaka, Japan
[6]Rinku General Medical Center, Izumisano, Osaka, Japan
[7]Department of Community Medicine, Osaka University Graduate School of Medicine, Suita, Osaka, Japan

Aim: A direct oral anti-coagulant, FXa inhibitor, has been applied to the clinical treatment of myocardial infarction (MI). Experimental studies in mice indicated that FXa inhibitors reduced atherosclerosis and prevented cardiac dysfunction after coronary ligation. These studies suggested that protease-activated receptor (PAR) 2, a major receptor of activated FX, may play an important role in atherosclerosis and cardiac remodeling.

Methods: The effects of a FXa inhibitor, rivaroxaban, were investigated in a new murine model of ischemic cardiomyopathy (ICM) using SR-BI KO/*ApoeR61*$^{h/h}$ mice (Hypo E mice) that developed MI by high-fat diet loading.

Results: Hypo E mice were fed rivaroxaban-containing (n=49) or control chow diets (n=126) after the induction of MI. The survival curve of the rivaroxaban-treated group 2 weeks after the induction of MI was improved significantly as compared with the non-treatment group (survival rate: 75.5% vs. 47.4%, respectively, p=0.0012). Echocardiography and the expression of BNP showed that rivaroxaban attenuated heart failure. Histological analyses revealed that rivaroxaban reduced aortic atherosclerosis and coronary occlusion, and markedly attenuated cardiac fibrosis. Rivaroxaban treatment decreased cardiac PAR2 levels and pro-inflammatory genes.
In vitro, rivaroxaban application demonstrated the increase of cell viability against hypoxia in cardiac myocytes and the reduction of hypoxia-induced inflammation and fibrosis-related molecules in cardiac fibroblasts. The effects of the PAR2 antagonist against hypoxia-induced inflammation were comparable to rivaroxaban in cardiac fibroblasts.

Conclusions: Rivaroxaban treatment just after MI in Hypo E mice prevented the progression of ICM by attenuating cardiac remodeling, partially through the suppression of the PAR2-mediated inflammatory pathway.

Key words: Ischemic cardiomyopathy, Atherosclerosis, Protease-activated receptor 2, Cardiac remodeling, Rivaroxaban

Introduction

Recent advances in coronary intervention have reduced early death due to myocardial infarction (MI)[1]; however, survivors with multiple coronary lesions often suffer from chronic heart failure (CHF) due to ischemic cardiomyopathy (ICM)[2]. Atherosclerosis and cardiac remodeling are important pathologi-

Address for correspondence: Shizuya Yamashita, Department of Cardiovascular Medicine, Osaka University Graduate School of Medicine, 2-2 Yamadaoka, Suita, Osaka, 565-0871, Japan E-mail: shizu@imed2.med.osaka-u.ac.jp

Received: December 4, 2018 Accepted for publication: January 17, 2019

cal bases in ICM. Many cellular and molecular pathways contribute to ICM. Several coagulation proteases and protease-activated receptor (PAR)-mediated pathways may serve as underlying mechanisms.

PARs are a family of G protein-coupled, seven transmembrane domain receptors that are activated by the proteolytic cleavage of the receptor N-terminus by several proteases, generating a novel tethered ligand, which subsequently activates the receptor by intramolecular binding[3]. Among the four subtypes of the PAR family, as demonstrated in recent studies, PAR2 is distributed in several cell types (i.e., endothelial cells, smooth muscle cells, and leukocytes) and contributes to the development of inflammatory diseases[4], immune responses[5], proliferation, cardiomyopathy, and heart remodeling[6]. PAR2 signaling was shown to be involved in lung and renal fibrosis, vascular remodeling, and atherosclerosis[7, 8]. However, the role of PAR2 in the development of cardiac remodeling has not been elucidated fully.

Direct oral anti-coagulants, FXa inhibitors, have been applied to the treatment of MI. Clinical trials indicated that rivaroxaban reduced the risk of composite death from cardiovascular causes, myocardial infarction, or stroke in patients with a recent acute coronary syndrome (ACS)[9]. Experimental studies in mice indicated that FXa inhibitors reduced atherosclerosis[10] and prevented cardiac dysfunction after coronary ligation[11]. These studies suggested that PAR2 may play an important role in atherosclerosis and cardiac remodeling.

Previously, we established a new murine model of ICM[12] using SR-BI KO/*ApoeR61*$^{h/h}$ mice (Hypo E mice) that developed MI after high-fat diet loading. In this study, we elucidated the effects and mechanism of a FXa inhibitor, rivaroxaban, on atherosclerosis and cardiac remodeling in ICM model mice and *in vitro* studies, especially focused on PAR2.

Methods

Animals and Diets

SR-BI KO/*ApoeR61*$^{h/h}$ mice (mixed C57BL/6 x 129 background) were obtained as a gift from Monty Krieger, Biology Department, Massachusetts Institute of Technology (Cambridge, MA, USA). Male mice were weaned at 4 weeks of age and housed in a barrier facility under specific pathogen-free conditions, with a 12-hour light/12-hour dark cycle. At 8 weeks of age, the mice were fed a Paigen diet for 7 days to induce ICM model mice; after 7 days' of the Paigen diet, mice were fed a chow diet with or without rivaroxaban (10 mg/kg body weight/day) for 2 weeks. Previous reports used various doses of rivaroxaban in mice[13-17]. ICM might be prevented partially by the inhibition of microvascular thrombus formation. Doses of 5 mg/kg rivaroxaban did not inhibit FXa activity in mice[10]. Although FXa activity was not examined, a high dose of 10 mg/kg rivaroxaban might inhibit microvascular thrombus in mice[15]. All mice at 11 weeks of age were euthanized with pentobarbital (120 mg/kg, intraperitoneally) and tissues and blood samples were collected.

The Paigen diet, containing 1.25% cholesterol, 7.5% cocoa butter, and 0.5% sodium cholate, was produced by Oriental Yeast Co., Ltd., Tokyo, Japan. The caloric composition of this diet was 21.4% protein, 27.4% fat, and 51.2% carbohydrate. The original Paigen diet was described previously[18, 19]. In contrast, the caloric composition of the normal chow diet (MF diet, Oriental Yeast Co., Ltd.) was 12.8% fat, 25.6% protein, and 61.6% carbohydrate. Rivaroxaban was supplied by Bayer Pharma AG.

Previous studies indicated that female SR-BI KO/*ApoeR61*$^{h/h}$ mice are infertile[20]. Thus, female *ApoeR61*$^{h/h}$ mice with heterozygous null mutations in SR-BI were mated with male SR-BI KO/*ApoeR61*$^{h/h}$ mice[20]. The genotypes were detected by polymerase chain reaction as described previously[21, 22].

All experimental procedures conformed with the guidelines of the Animal Research Committee of Osaka University. The protocol was approved by the Animal Care and Use Committee of the Osaka University Graduate School of Medicine.

Echocardiography

Ultrasonography (Vevo770, VisualSonics, Inc., Toronto, Canada) was performed using a 25-MHz linear transducer (VisualSonics) on conscious mice. The heart was imaged on a two-dimensional parasternal long-axis view, and an M-mode echocardiogram of the mid-ventricle was recorded at the papillary muscle level.

Morphological and Biochemical Analyses

The heart and ascending aorta of the mouse were perfused with phosphate-buffered saline (PBS) containing 1% heparin, via the left ventricular apex. The hearts of the mice were isolated and fixed with formalin. Paraffin sections (10 μm) of hearts were stained with Masson's trichrome (Sigma-Aldrich, St. Louis, MO, USA) to evaluate the fibrotic area.

Frozen sections of the aortic root at the level of the aortic valve were stained with oil red O and counterstained with hematoxylin. The atherosclerotic lesions were calculated as the average of oil red O positive–stained areas in at least eight slices of each mouse, using Image J software.

Paraffin sections of the mid-ventricle were

stained with hematoxylin–eosin (HE). Randomly selected microscopic fields ($n=10$) per mouse were evaluated to calculate the percentage of occluded coronary arteries/total arteries. The evaluation of various extents of coronary artery occlusion is shown in **Supplemental Fig. 1**.

Blood was collected at the time of sacrifice with an overdose of pentobarbital. Plasma was separated by centrifugation and stored at −80℃ until required. Plasma concentrations of triglyceride and total cholesterol were determined with commercially available kits according to the manufacturers' instructions (Wako Diagnostics).

Isolation and Cell Culture of Neonatal Rat Cardiac Myocytes and Cardiac Fibroblasts

Cardiac myocytes (CMs) were prepared from 1 to 3-day-old Sprague-Dawley rats and cultured as described previously[23]. Briefly, hearts were removed and minced in PBS and digested with trypsin; after digestion, cells were seeded onto uncoated plastic dishes and incubated for 60 min at 37℃. The supernatant (containing the CMs) and the attached cells (containing primary rat cardiac fibroblasts [FBs]) were collected and maintained in Dulbecco's Modified Eagle's Medium (DMEM) supplemented with 10% fetal bovine serum (FBS), penicillin (100 U/ml), and streptomycin (100 mg/ml) at 37℃ in 5% CO_2. The medium was changed every other day and 90% confluent cells were used for experiments. FBs within the second passage were used for experiments. To study the effect of rivaroxaban, CMs and FBs were treated with or without rivaroxaban dissolved in DMSO with 1% FBS for 12 or 24 hours.

Effects of Rivaroxaban Against Hypoxic Stress *in Vitro*

Rat neonatal CMs and FBs were incubated in an anaerobic container with an Anaero Pack (Mitsubishi Gas Chemical)[24] to induce hypoxic stress. The percentage of O_2 in the jar after 2 hours with the Anaero Pack was under 0.1%. The cells were starved for 24 hours in serum-free DMEM; later, cells were incubated in fresh medium with or without rivaroxaban under hypoxic stress. After hypoxic stimulation, cells were harvested for quantitative real-time polymerase chain reaction (qPCR) measurement and protein isolation.

Reverse Transcription, Real-Time Polymerase Chain Reaction

Total RNA was extracted from tissues and cells. RNA was DNase-treated using SuperScript VILO (SuperScript VILO cDNA Synthesis Kit, Life Technologies Co., Carlsbad, CA, USA). Reverse transcription was performed using the QuantiTect Reverse Transcription Kit (QIAGEN, Hilden, Germany). qPCR was performed with SYBR Green (QuantiTect SYBR Green PCR kit, Qiagen). Relative levels of genes were expressed in arbitrary units, which were normalized to the level of mouse GAPDH expression. *In vitro*, the gene expression of hypoxia-conditioned cells was normalized to the level of rat β-actin gene expression. Gene-specific primers are shown in **Supplemental Tables 1** and **2**.

Western Blot

Equal amounts of total protein were resolved by sodium dodecyl sulfate polyacrylamide gel electrophoresis, and were then electrophoretically transferred to polyvinylidene fluoride membranes (Bio-Rad, Hercules, CA, USA). The membrane was blocked with 5% skim milk powder in Tris-buffered saline (TBS)-Tween for 1 hour and incubated with primary antibodies at 4℃ overnight. The membrane was washed in TBS-Tween and incubated with a secondary antibody conjugated to horseradish peroxidase for 1 hour and subjected to enhanced chemiluminescence (GE Healthcare). The following antibodies were used: PAR2 (Abcam) and GAPDH. GAPDH was used as an interval control.

Cell Viability Assay (MTT Assay)

Cell viability was evaluated by the conventional 3-(4, 5-dimethylthiazol-2-yl)-2, 5-diphenyl-tetrazolium bromide (MTT) reduction assay. In this assay, viable cells convert MTT to insoluble blue formazan crystals by the mitochondrial respiratory chain enzyme succinate dehydrogenase. Cells seeded at a density of $2.5\times10^4/cm^2$ in 96-well plates were treated with or without rivaroxaban (0.1, 0.5, 2, and 5 μg/ml) for 24 hours under hypoxic conditions. Absorbance was monitored at 570 nm.

Apoptosis Assay

The anti-apoptotic effect of rivaroxaban on CMs was detected by the TUNEL assay. CMs were plated on glass-bottom dishes (0.7×10^5 cells per well) and starved in serum-free medium for 24 hours. Then cells were exposed to hypoxic conditions with or without rivaroxaban. The TUNEL assay was conducted according to the manufacturer's instructions (Invitrogen) to detect apoptotic nuclei. Total nuclei were stained by 4′,6-diamidino-2-phenylindole. Randomly selected microscopic fields ($n=10$) were evaluated to calculate the ratio of TUNEL-positive cells to total cells.

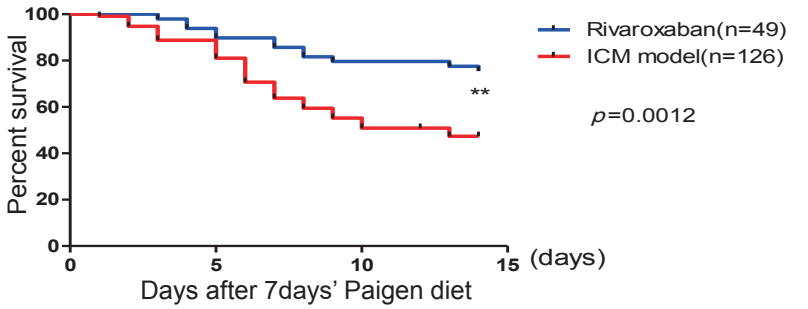

Fig. 1. Rivaroxaban treatment significantly improved the survival rate

The survival rate of the rivaroxaban-treated group improved significantly compared with the non-treated ICM model (rivaroxaban group, $n=49$; ICM model group, $n=126$). $^{**}p<0.01$.

Statistical Analysis

Results are expressed as the mean ± standard error of the mean. Paired data were evaluated using Student's *t*-test. Differences between multiple groups were compared by one-way analysis of variance, followed by Bonferroni post hoc testing. Survival analysis was evaluated by the Kaplan–Meier method with a log-rank test. A value of $p<0.05$ for differences was considered statistically significant.

Results

Rivaroxaban Treatment Significantly Improved the Survival Rate and Suppressed the Progression of Heart Failure in ICM Model Mice

After 7 days of Paigen diet loading, Hypo E mice were fed rivaroxaban or not for 2 weeks; the survival rate of the rivaroxaban-treated group was significantly improved compared with the non-treatment group (75.5% vs 47.4%, respectively, $p=0.0012$) (**Fig. 1**). Beyond the observation period, the life spans of six rivaroxaban-treated mice were examined. The life spans were 206, 206, 196, 192, 164, and 164 days. The heart weight/body weight ratio ($p<0.001$), heart weight/tibia length ratio ($p<0.05$), lung weight/body weight ratio ($p<0.001$), and lung weight/tibia length ratio ($p<0.01$) were decreased significantly (**Fig. 2A**). There were no differences between both groups in total cholesterol, triglycerides, red blood cell, and platelet counts (data not shown). Echocardiography indicated that rivaroxaban inhibited the deterioration of heart failure compared with the non-treatment group (**Fig. 2B**). Fraction shortening was increased markedly in the treated group compared with the non-treatment group (36.2 ± 4.5% vs. 57.6 ± 1.7%, respectively, $p<0.001$) (**Fig. 2B**). Representative photographs (**Fig. 3B** and **Supplemental Fig. 1**) showed that many clear cells, like foam cells, occluded the coronary arteries. The center of the coronary arteries with an accumulation of clear cells was sometimes occluded by the thrombus. There were no differences in the heart rate. The mRNA expression of BNP ($p<0.05$) and ANP ($p<0.01$) (**Fig. 2C**) was also consistently alleviated by rivaroxaban treatment. These results indicated that rivaroxaban treatment attenuated the deterioration of heart failure and increased the survival rate without altering lipid levels or blood cell counts.

Rivaroxaban Alleviated Aortic Atherosclerosis, Occlusion of Coronary Arteries, and Inflammation in ICM Model Mice

Rivaroxaban treatment alleviated atherosclerotic plaque areas in the aortic root in the treated group compared with the non-treatment group, as observed by oil red O staining (18.06 ± 3.16 vs. 8.47 ± 1.57 ($\times 10^4$ μm^2) respectively, $p<0.05$) (**Fig. 3A**).The percentage of occluded coronary arteries was attenuated by rivaroxaban treatment compared to the controls, as observed by HE staining (68.52 ± 2.98% vs. 41.82 ± 6.02%, $p<0.001$) (**Fig. 3B**). The cardiac mRNA expression levels of inflammation-related genes of IL-1β, IL-6, NF-κB, and TNF-α demonstrated a reduction by rivaroxaban treatment (**Fig. 3C**). IL-6 and NF-κB indicated significant differences ($p<0.05$ and $p<0.01$, respectively). These results revealed that rivaroxaban reduced inflammation and atherosclerosis in ICM model mice.

Rivaroxaban Attenuated Cardiac Fibrosis and Decreased mRNA Expression of Fibrosis-Related Genes in ICM Model Mice

Cardiac fibrosis was estimated by Masson's staining. Fibrotic areas were reduced significantly by rivaroxaban treatment compared to controls (15.59 ±

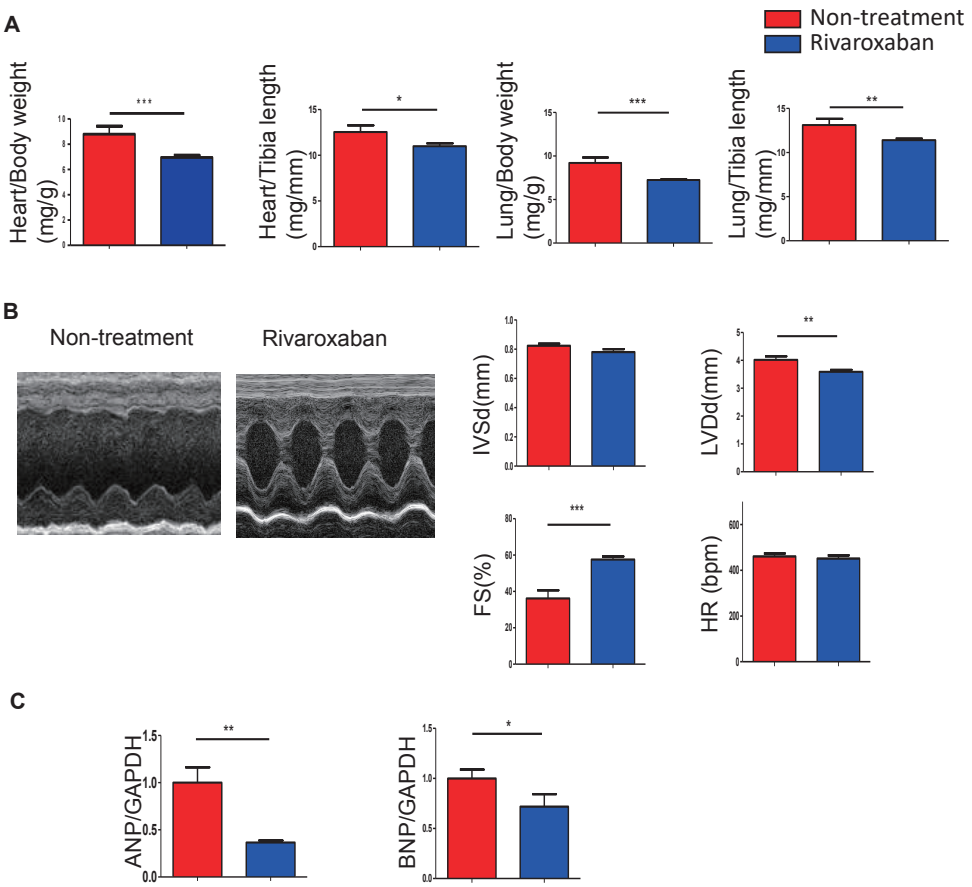

Fig. 2. Rivaroxaban suppressed the progression of heart failure in ICM model mice

(A) The heart weight/body weight ratio, heart weight/tibia length ratio, lung weight/body weight ratio, and lung weight/tibia length ratio were decreased significantly ($n=11$–30 per group). (B) Echocardiography showed that fraction shortening in the rivaroxaban-treated group was prevented remarkably compared with the non-treated group ($n=10$–11). (C) The mRNA expression of ANP and BNP was decreased markedly ($n=5$–8). $^{*}p<0.05$, $^{**}p<0.01$, and $^{***}p<0.001$.

2.93% vs. 4.06±1.37%, respectively, $p<0.01$) (**Fig. 4A**). The mRNA expression of fibrosis-related genes, such as MMP9, MMP12, TIMP1, TGF-β, collagen-1, and collagen-3, was decreased by rivaroxaban treatment (**Fig. 4B**). Among these genes, MMP12 ($p<0.05$), TIMP1 ($p<0.05$), collagen-1 ($p<0.01$), and collagen-3 ($p<0.01$) indicated significant changes.

Cardiac Expression of PARs was Attenuated by Rivaroxaban Treatment in ICM Model Mice

The cardiac mRNA expression of PAR1 and PAR2 was increased in the ICM model with the Paigen diet as compared with non-MI mice with the normal chow diet. The increase of PAR1 and PAR2 was attenuated markedly by rivaroxaban treatment (**Fig. 5A**). Consistent with the results of mRNA, the PAR2 protein also showed a significant reduction by rivaroxaban treatment (**Fig. 5B**), whereas the PAR1 protein showed no decrease by the treatment (**Fig. 5B**).

In CMs, Rivaroxaban Improved Cell Viability and Decreased Apoptosis against Hypoxic Exposure for 24 Hours

To clarify the mechanism of rivaroxaban on cardiac remodeling, rat neonatal CMs were exposed to hypoxic conditions for 12 or 24 hours, with or without rivaroxaban. The MTT assay revealed that the viability of CMs was dose-dependently increased by rivaroxaban treatment for 12 and 24 hours under hypoxia (**Fig. 6A**). Apoptotic cells were reduced by rivaroxaban treatment for 24 hours under hypoxia (**Fig. 6B**). The results suggest a cardioprotective role of rivaroxaban in the progress of ICM.

Consistent with experiments *in vivo*, the results of qPCR analyses demonstrated that hypoxia stimulation induced high mRNA expression of PAR1 and

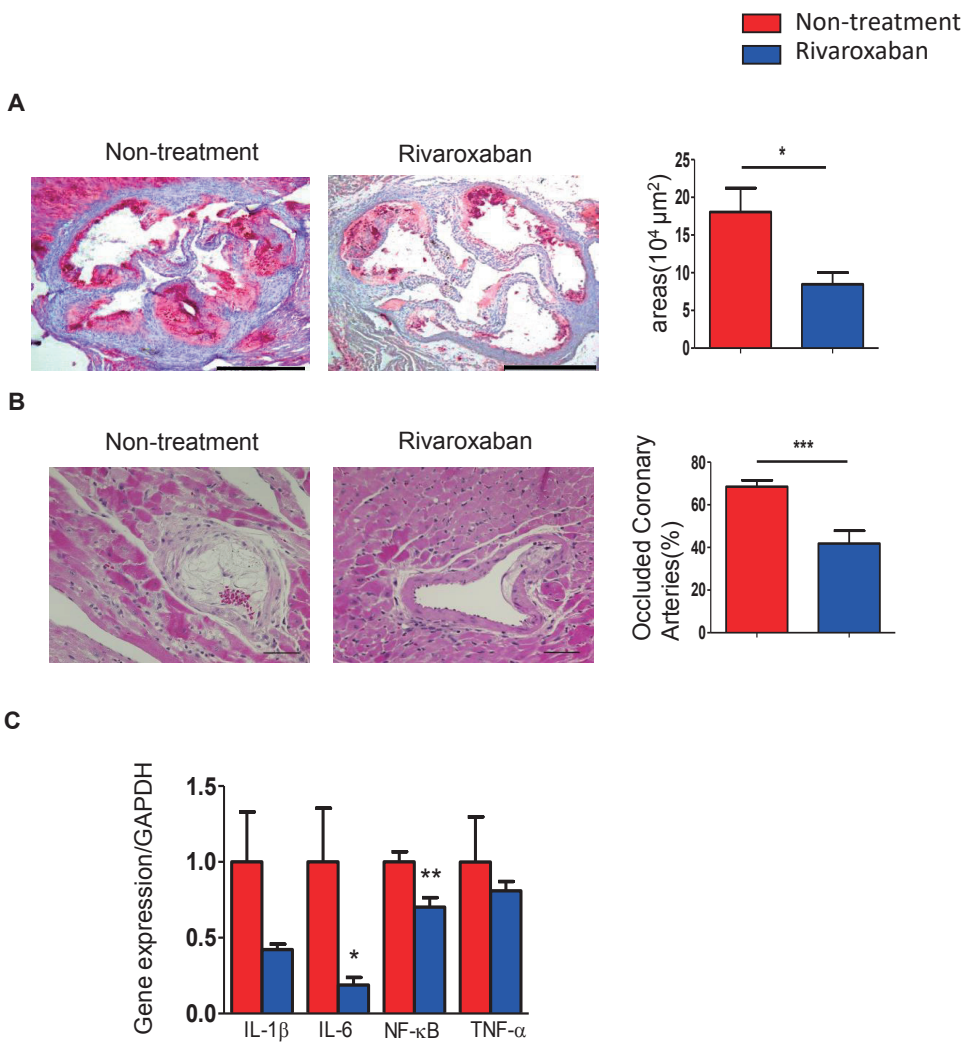

Fig. 3. Effects of rivaroxaban on atherosclerosis in the aortic root and on occluded coronary arteries in ICM model mice

Rivaroxaban alleviated atherosclerosis and occluded coronary arteries in ICM model mice.
(A) Representative images of oil red O staining of atherosclerotic plaques in aortic roots. Rivaroxaban treatment alleviated lipid deposition as compared with the non-treated group ($n=5$–7; bar = 500 μm). (B) HE staining indicated that occluded coronary arteries were decreased by rivaroxaban treatment compared with the non-treated group ($n=11$–14; bar = 50 μm). (C) The mRNA expression of pro-inflammatory genes revealed that rivaroxaban decreased the inflammatory molecules in the heart ($n=8$–9). *$p<0.05$, **$p<0.01$, and ***$p<0.001$.

PAR2, and the high PAR1 and PAR2 levels were decreased by rivaroxaban treatment (Fig. 7A). Meanwhile, hypoxia induced high mRNA expression of inflammatory molecules IL-6, IL-1β, and TNF-α. IL-6 and IL-1β were decreased significantly after rivaroxaban treatment ($p<0.05$) (Fig. 7C). The protein level of PAR2 was not decreased significantly by rivaroxaban (Fig. 7B). The reason for this may be that PAR2 expression in CMs is very low.

In FBs, Rivaroxaban Attenuated the Expression of PAR2 and Inflammation against Hypoxic Exposure for 24 Hours

To investigate the potential molecular mechanism by which rivaroxaban prevented cardiac fibrosis, the effects of rivaroxaban on the proliferative ability and inflammatory responses under hypoxic conditions were examined. The MTT assay revealed that rivaroxaban did not affect the proliferation of FBs under hypoxic conditions for 24 or 48 hours (Fig. 8A). Riva-

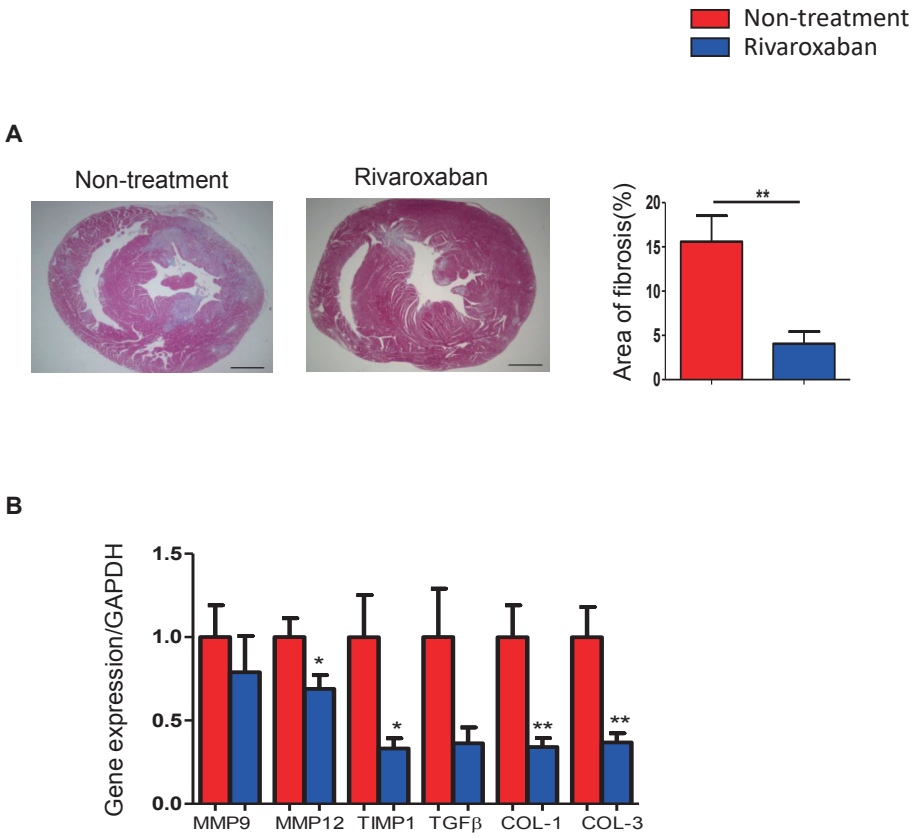

Fig. 4. Rivaroxaban treatment attenuated cardiac fibrosis in ICM model mice

(A) Masson's staining showed that fibrotic areas were significantly alleviated by rivaroxaban treatment ($n=7$–11; bar=1 mm). (B) The mRNA expression of fibrosis-related genes was decreased by rivaroxaban treatment ($n=8$). *$p<0.05$, **$p<0.01$

roxaban suppressed mRNA expression and the protein level of PAR2 in FBs under hypoxic conditions (**Fig. 8B, C**). The mRNA expression of fibrosis-related genes MMP9 ($p<0.01$) and COL-1 ($p<0.01$) were significantly lower in the presence of rivaroxaban (**Fig. 9B, C**). Pro-inflammatory genes of IL-6 ($p<0.05$), IL-1β, and TNF-α were decreased simultaneously (**Fig. 9D-F**).

PAR2 Antagonist Attenuated Pro-Inflammatory and Fibrosis-Related Molecules in Cardiac Fibroblasts against Hypoxic Exposure for 24 Hours

To clarify whether PAR2 inhibition reverses inflammation and fibrosis in FBs, we performed the in vitro experiment using FBs exposed to hypoxia treated with or without a PAR2 antagonist: FSLLRY (10 μM) for 24 hours or rivaroxaban (2 μg/ml) for 24 hours or FSLLRY (10 μM) for 24 hours, subsequently changed to rivaroxaban (2 μg/ml) for 24 hours. Hypoxia-induced high expression of PAR2; both rivaroxaban and FSLLRY inhibited PAR2 expression (**Fig. 9A**). Hypoxia caused the increased expression of fibrosis-related and pro-inflammatory genes. The PAR2 antagonist treatment significantly attenuated the expression of fibrosis-related molecules MMP9 ($p<0.01$) and COL-1 ($p<0.05$) (**Fig. 9B, C**), and reduced the expression of the pro-inflammatory gene IL-6 ($p<0.05$) (**Fig. 9D**). The PAR2 antagonist also showed a tendency to reduce the expression of IL-1β and TNF-α (**Fig. 9E, F**). The suppressive effect is consistent with the effect of rivaroxaban treatment. Furthermore, in case FBs were blocked by the PAR2 antagonist in advance, no further decrease of pro-inflammatory and fibrosis-related molecules was observed by subsequent rivaroxaban treatment. Collectively, these results revealed that rivaroxaban plays an anti-inflammatory and anti-fibrotic role in cardiac FBs against hypoxic exposure probably via the PAR2 pathway.

Discussion

In the present study, the presence of PAR2 was confirmed in the heart of mice and rats. The PAR2

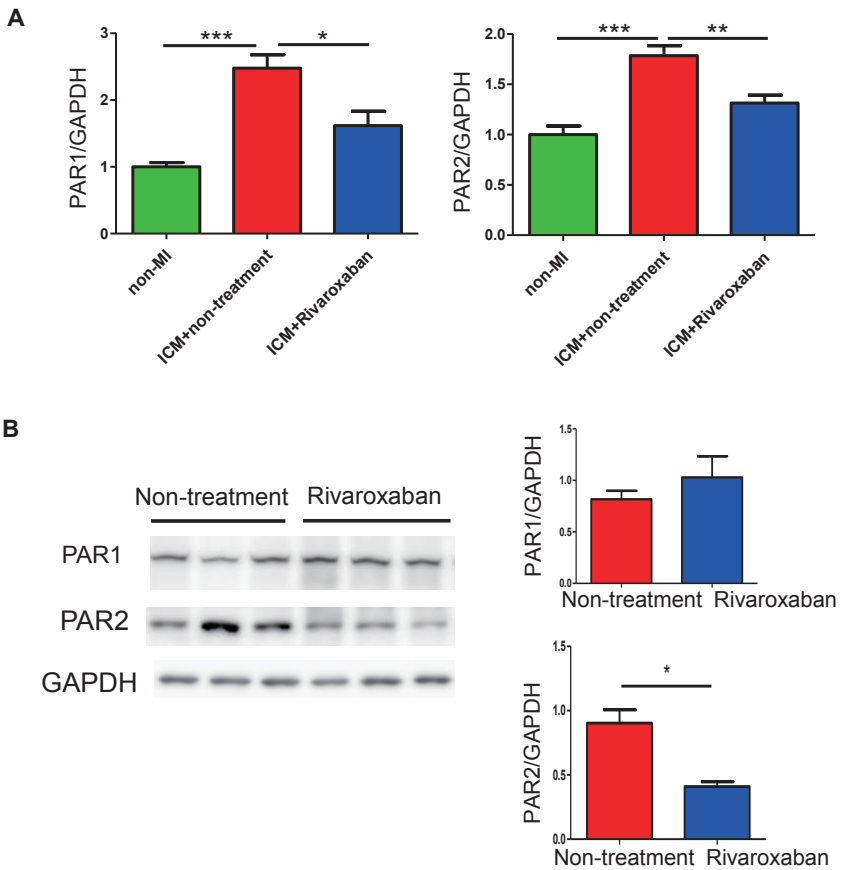

Fig. 5. Cardiac PAR expression in non-MI mice, ICM mice, and rivaroxaban-treated ICM mice

(A) The mRNA expression levels of PAR2 and PAR1 were significantly upregulated after a high-fat diet administration and downregulated markedly by rivaroxaban treatment ($n=5$–8). (B) The protein level of PAR2 was reduced by rivaroxaban treatment consistently ($n=4$). $^{*}p<0.05$, $^{**}p<0.01$, and $^{***}p<0.001$.

level was upregulated in ICM model mice and was reduced remarkably by the FXa inhibitor rivaroxaban (**Fig. 5A**). FXa induces PAR2 expression, and the inhibition of FXa caused a reduction of PAR2[10, 25]. In neonatal rat CMs and cardiac FBs, PAR2 levels were increased under hypoxic exposure (**Figs. 7** and **8**). PAR2 is reportedly also expressed in humans[6]. These findings suggest that PAR2 may contribute to ischemic heart failure in humans.

Importantly, rivaroxaban treatment markedly improved the survival rate of CHF just after the induction of MI (**Fig. 1**). This may be due to the attenuation of atherosclerotic plaque progression and the prevention of cardiac fibrosis by rivaroxaban treatment (**Figs. 3A** and **4A**). The attenuation of atherosclerosis was already confirmed by the work of others in atherosclerosis model mice[4, 10, 26]. In particular, the effect of rivaroxaban on the reduction of fibrotic areas in the heart was extremely obvious in our experiment (**Fig. 4**). A previous study showed that PAR2 deficiency reduced the initial infarct size of the heart in the mice model of ischemia/reperfusion injury[6].

Accumulating evidence shows that PARs play important roles in cardiovascular physiology and pathophysiology[27]. PAR2 participates in fibrosis. It is reported that tryptase can accelerate the progress of cardiac fibrosis by a mechanism of PAR2 activation[28]. Borensztajn *et al.* showed that FXa-dependent PAR2 cleavage might play a role in the progression of tissue fibrosis and remodeling in wound healing[29]. FXa induces fibrosis via thrombin generation or via PAR2-dependent signaling; PAR2 signaling leads to the secretion of fibrosis-related factors MCP-1, IL-6, and TGF-β[29]. The expression and secretion of IL-6 are associated with fibrosis in the lung[30], liver[31], and skin[32]. In our study, IL-6 may play a role in fibrosis and inflammation *in vivo* and *in vitro* (**Figs. 3, 7**, and **9**). PAR2 may contribute to ICM, partly by attenuat-

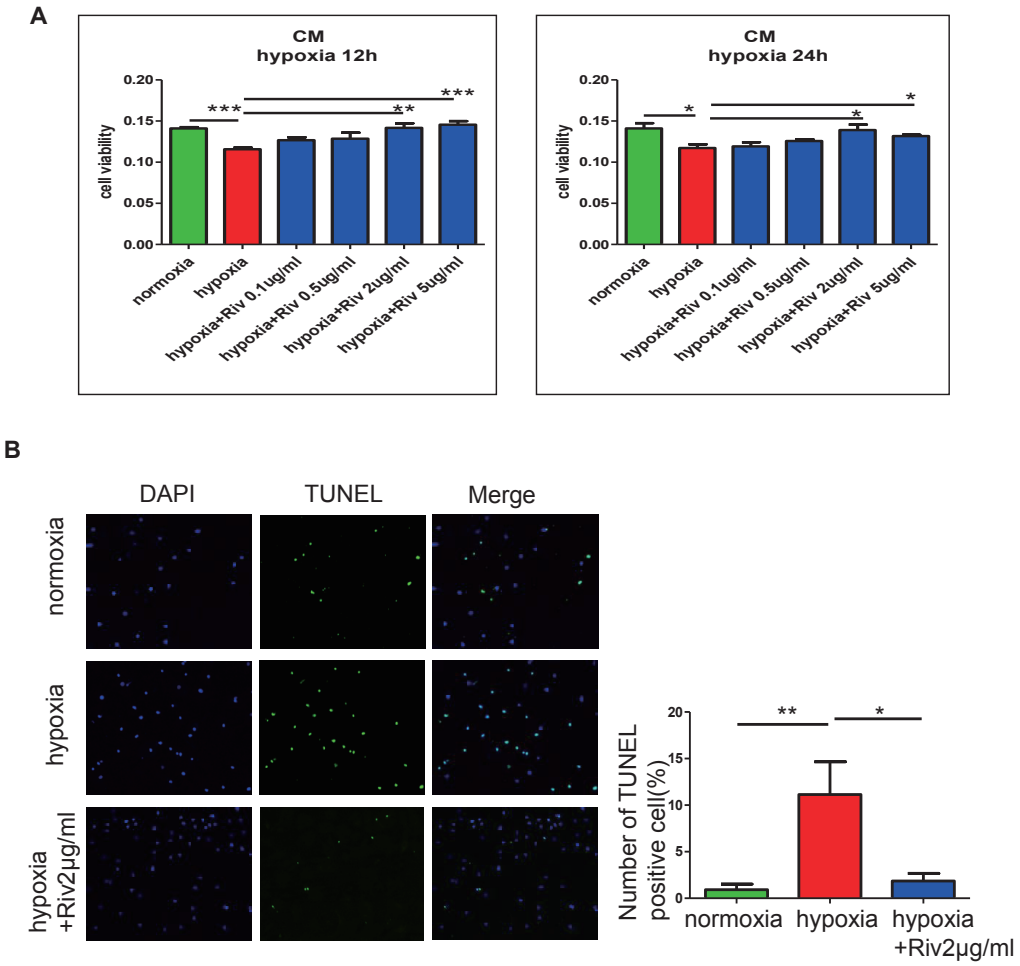

Fig. 6. Effects of rivaroxaban in cardiac myocytes *in vitro*

(A) Hypoxic stimulation induced a decrease in the cell viability of CMs. The cell viability of CMs under hypoxia was dose-dependently improved by the presence of rivaroxaban for 12 and 24 hours ($n=4$–5 per group). (B) Hypoxic stimulation caused the apoptosis of CMs. The apoptotic CMs were reduced remarkably after rivaroxaban treatment for 24 hours. The ratio of TUNEL-positive cells/total cells (%) was calculated in 10 areas under a microscope and averaged. $^{*}p<0.05$, $^{**}p<0.01$, and $^{***}p<0.001$. Riv: rivaroxaban.

ing inflammation.

In addition, our *in vitro* experiment elucidated the protective role of rivaroxaban against hypoxia-induced inflammation (**Figs. 7** and **9**). Kwapiszewska *et al.* reported the attenuating role of vascular remodeling in the lung and that PAR2$^{-/-}$ mice were protected against hypoxia-induced pulmonary hypertension[8]. Whether the pathway is functional in cardiac FBs under hypoxia has not been investigated clearly. Our study showed PAR2 expression and function in isolated cardiac FBs against hypoxic exposure (**Fig. 8**). Hypoxia induced a remarkable increase of PAR2 expression in FBs, which was attenuated by co-incubation with the PAR2 inhibitor peptide FSLLRY or FXa inhibitor rivaroxaban (**Fig. 9**). Collectively, hypoxia-induced changes in cardiac FBs were mediated by the PAR2-dependent pathway. Rivaroxaban may play a cardioprotective role at least partially by anti-inflammation and anti-fibrosis in the progression of cardiac remodeling.

Rivaroxaban was also shown to have a cardiac protective role by anti-apoptosis in CMs. PAR2 deletion inhibited NF-κB signaling[4]. The inhibition of NF-κB activation may be involved in the underlying mechanism. There are reports that PAR2 activation leads to the generation of nitric oxide and reactive oxygen species (ROS)[33, 34]. The anti-apoptotic role of rivaroxaban may be mediated by suppressing ROS under hypoxia stress.

Rivaroxaban has been shown to be an effective therapeutic agent in preventing stroke and systemic embolism events in patients with atrial fibrillation[35]

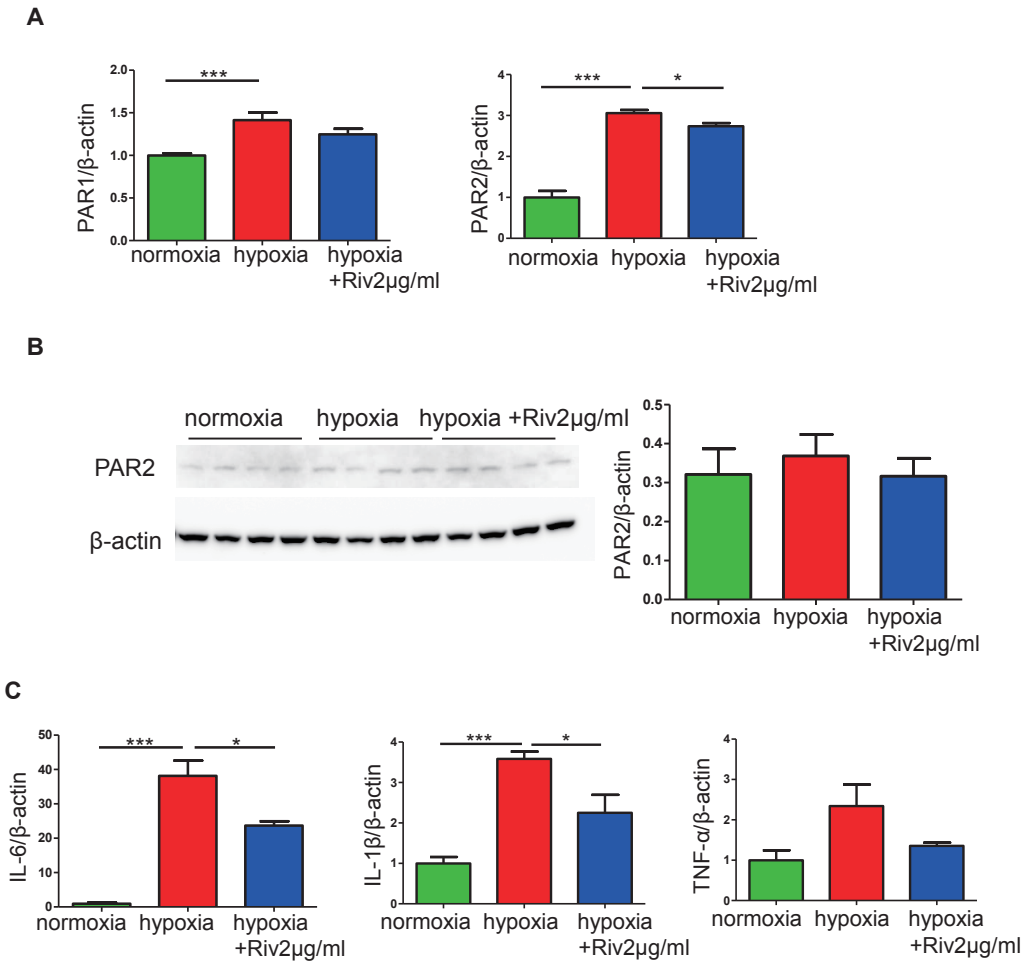

Fig. 7. Effects of rivaroxaban on PAR1, PAR2, and inflammation genes in cardiac myocytes

(A) The mRNA expression levels of PAR1 and PAR2 in CMs were increased after stimulation under hypoxia for 24 hours. Rivaroxaban treatment reduced both PAR1 and PAR2, and PAR2 significantly ($n=4$–6 per group). (B) Protein levels of PAR2 in CMs showed no significant changes ($n=3$–4 per group). (C) The mRNA expression levels of pro-inflammatory genes in CMs were decreased significantly ($n=3$–4 per group). $^{*}p<0.05$ and $^{***}p<0.001$. Riv: rivaroxaban.

and in treating symptomatic pulmonary embolism[36] and symptomatic venous thrombosis[37]. Beyond anticoagulation therapy, rivaroxaban is also used for antithrombotic treatment following ACS[9]. Rivaroxaban-treated patients with stable coronary artery disease demonstrated that rivaroxaban lowered major vascular events and has the potential to reduce morbidity and mortality from coronary artery disease[38]. Rivaroxaban is highly effective in venous thromboembolism, but the evidence regarding clinical questions and its basic mechanism are insufficient[39]. Our results may supply an additional explanation to these trials. However, a recent study of the COMMANDER HF Clinical Trials showed that 2.5 mg rivaroxaban twice daily did not have a significantly lower rate of death, myocardial infarction, or stroke than the placebo among patients with worsening CHF, reduced left ventricular ejection fraction, coronary artery disease, and no atrial fibrillation[40]. In comparison with our research, this suggests that rivaroxaban may play an effective role in ICM in the early phase after MI, but may not be so effective in CHF.

There are several limitations to our study. First, rivaroxaban inhibits FX activation, and the exact mechanism of rivaroxaban on PARs has not been detected. Second, PAR2 expression in inflammatory cells, such as macrophages, smooth muscle cells, and epithelial cells, was not determined, and these cells may also contribute to cardiac remodeling. Third, cardiac diastolic function is a critical measurement in the progression of cardiac fibrosis[41], but it was not measured due to our technical limitation.

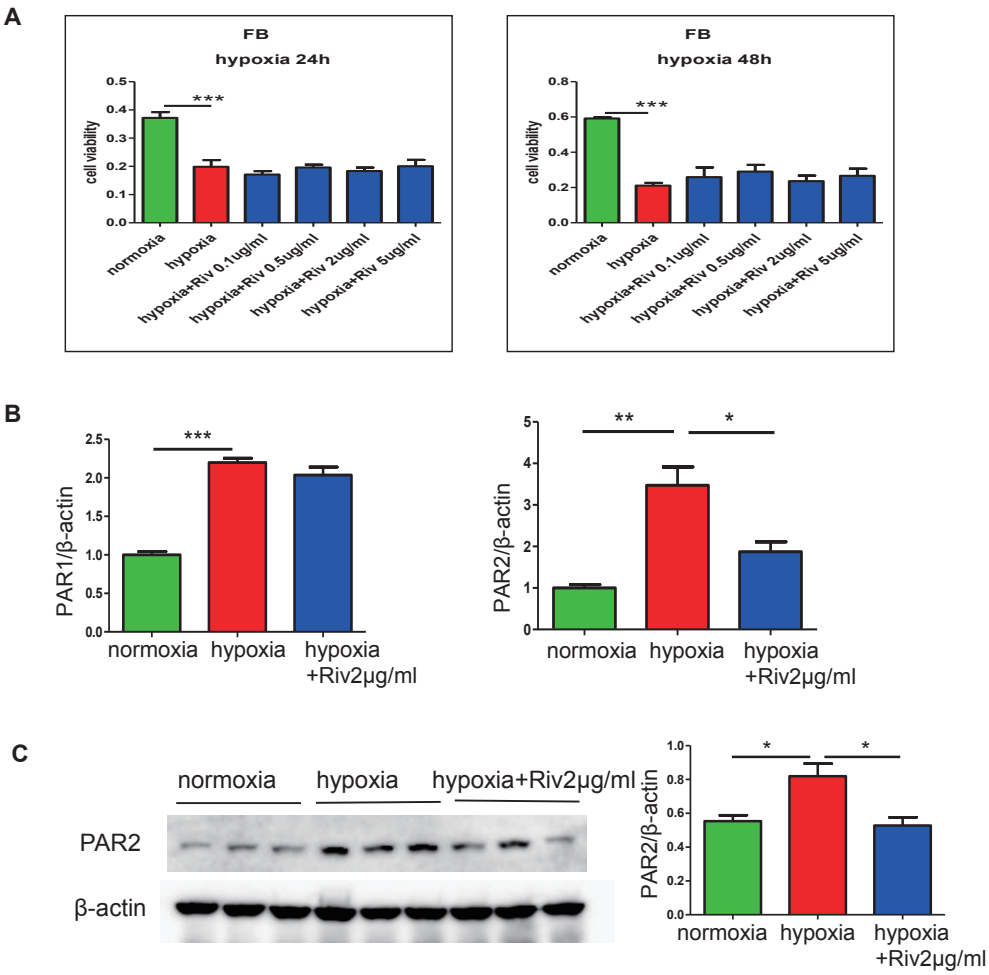

Fig. 8. Rivaroxaban downregulated the expression of PAR2 in cardiac fibroblasts

(A) The MTT assay demonstrated that hypoxic stimulation for 24 or 48 hours induced the reduction of proliferation of cardiac FBs. Rivaroxaban showed no effect on cell viability under hypoxic conditions for 24 or 48 hours ($n=5$–6 per group). (B) The results of qPCR analysis demonstrated that hypoxic stimulation for 24 hours increased the mRNA expression of PAR1 and PAR2, which were decreased by the presence of rivaroxaban, significantly in PAR2 ($n=3$). (C) The expression of the PAR2 protein level in cardiac FBs was increased by hypoxic stimulation for 24 hours, and was suppressed remarkably by the presence of rivaroxaban ($n=3$). $^{*}p<0.05$, $^{**}p<0.01$, and $^{***}p<0.001$. Riv: rivaroxaban.

However, our study provides clear evidence that rivaroxaban treatment just after the induction of MI significantly improved the survival rate in ICM model mice. In this model, rivaroxaban suppressed atherosclerosis, coronary occlusion, and subsequent cardiac remodeling, and also suppressed the elevation of PAR2 and inflammation. Experiments *in vitro* revealed that rivaroxaban directly protected apoptosis in CMs, and directly suppressed PAR2, inflammation, and fibrosis in cardiac FBs against hypoxic stimulation.

Finally, coronary intervention sometimes fails to remedy ischemia, especially with multiple vessel occlusion. In this clinical setting, the use of the FXa inhibitor just after MI may inhibit the progression of ICM by the following mechanism. The anti-coagulant effect of rivaroxaban reduces additional thrombus formation and endothelial dysfunction, which lead to the progression of atherosclerosis and coronary occlusion. PAR2-mediated reduction of ROS by rivaroxaban[33, 34] may also attenuate atherosclerosis. The inhibition of coronary occlusion is a major mechanism of improved cardiac hypoxia, fibrosis, and the survival rate. However, the inhibition of fibrosis was more marked than the inhibition of coronary occlusion. The direct effect of rivaroxaban on cardiac cells under hypoxic conditions was the additional mechanism to inhibit cardiac fibrosis. A recent paper also showed that intermittent hypoxia-induced fibrosis was attenuated by a high dose of rivaroxaban[17].

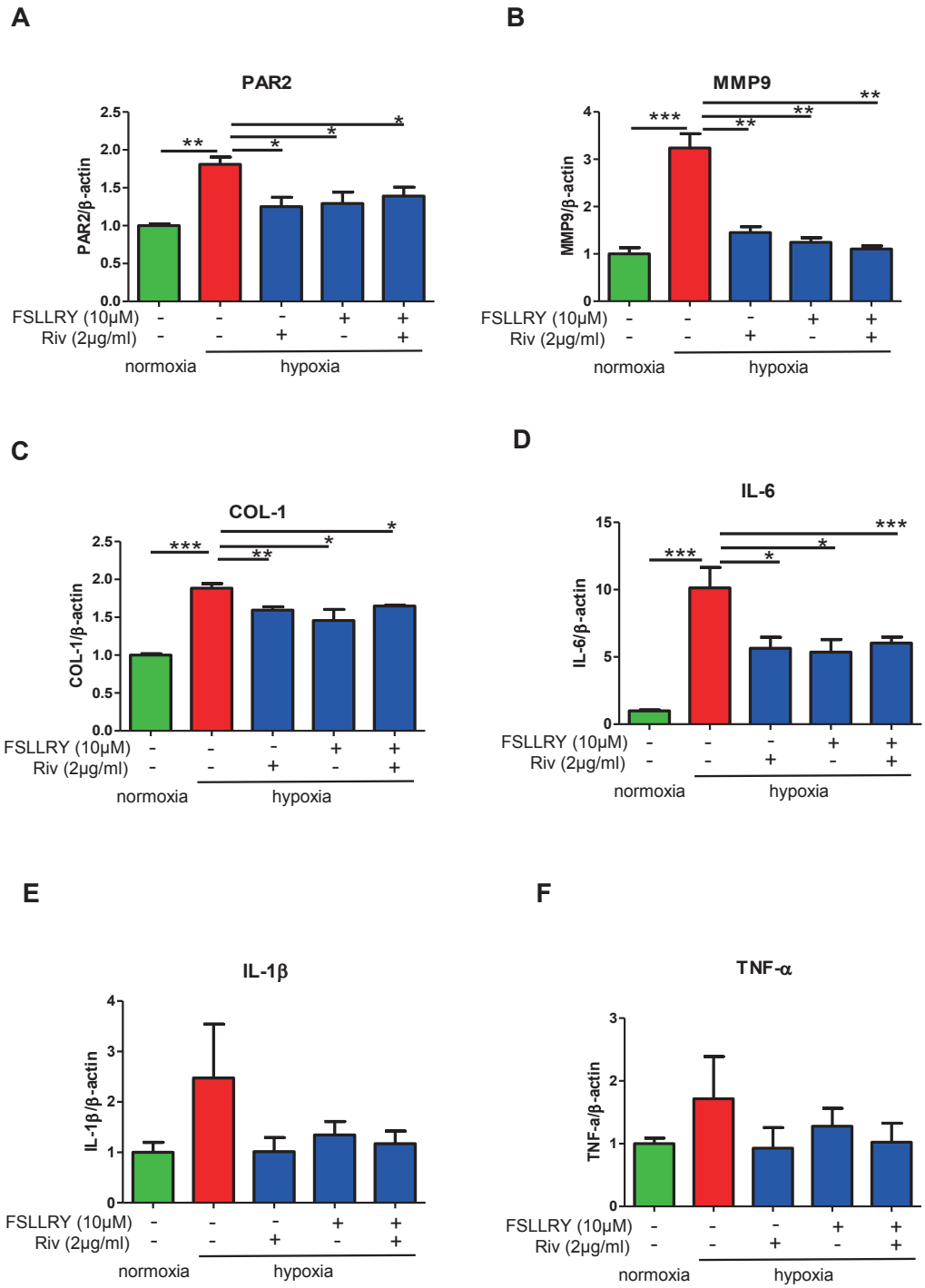

Fig. 9. Effects of rivaroxaban and a PAR2 antagonist on fibrosis and inflammation in cardiac fibroblasts

Cardiac FBs exposed to hypoxia were treated with or without a PAR2 antagonist, FSLLRY (10 μM) for 24 hours or rivaroxaban (2 μg/ml) for 24 hours or FSLLRY (10 μM) for 24 hours, subsequently changed to rivaroxaban (2 μg/ml) for 24 hours. (A) The elevated expression level of PAR2 induced by hypoxic stimulation was downregulated by rivaroxaban or the PAR2 antagonist FSLLRY, or both. (B, C) The mRNA expressions of MMP9 and COL-1 in cardiac FBs were attenuated by the presence of rivaroxaban or FSLLRY or both. (D–F) The mRNA expressions of pro-inflammatory genes IL-6, IL-1β, and TNF-α were reduced by the presence of rivaroxaban or FSLLRY or both (n=3–5 per group). *$p<0.05$, **$p<0.01$, and ***$p<0.001$. Riv: rivaroxaban.

Conclusion

In summary, our study presented evidence that rivaroxaban attenuates inflammation and fibrosis in the progression of cardiac remodeling. Rivaroxaban may function as an anti-inflammatory and anti-fibrotic agent, besides its anti-thrombotic role in the treatment of ICM just after MI. PAR2 may contribute as a potential target for the treatment of ICM.

Disclosures

Dr. Yamashita received research funding from Bayer Yakuhin, Ltd. The other authors declare that they have no conflicts of interests.

Acknowledgments

The authors thank Masumi Asaji, Ayami Saga, Takuya Kobayashi, and Misako Kobayashi for their technical assistance.

References

1) Levine GN, Bates ER, Blankenship JC, Bailey SR, Bittl JA, Cercek B, Chambers CE, Ellis SG, Guyton RA, Hollenberg SM, Khot UN, Lange RA, Mauri L, Mehran R, Moussa ID, Mukherjee D, Ting HH, O'Gara PT, Kushner FG, Ascheim DD, Brindis RG, Casey DE Jr, Chung MK, de Lemos JA, Diercks DB, Fang JC, Franklin BA, Granger CB, Krumholz HM, Linderbaum JA, Morrow DA, Newby LK, Ornato JP, Ou N, Radford MJ, Tamis-Holland JE, Tommaso CL, Tracy CM, Woo YJ, Zhao DX: 2015 ACC/AHA/SCAI Focused Update on Primary Percutaneous Coronary Intervention for Patients With ST-Elevation Myocardial Infarction. J Am Coll Cardiol, 2016; 67: 1235-1250
2) Ponikowski P, Voors AA, Anker SD, Bueno H, Cleland JGF, Coats AJS, Falk V, González-Juanatey JR, Harjola VP, Jankowska EA, Jessup M, Linde C, Nihoyannopoulos P, Parissis JT, Pieske B, Riley JP, Rosano GMC, Ruilope LM, Ruschitzka F, Rutten FH, van der Meer P: 2016 ESC Guidelines for the diagnosis and treatment of acute and chronic heart failure. Eur Heart J, 2016; 37: 2129-2200
3) Spronk HMH, De Jong AM, Crijns HJ, Schotten U, Van Gelder IC, Ten Cate H: Pleiotropic effects of factor Xa and thrombin: What to expect from novel anticoagulants. Cardiovasc Res, 2014; 101: 344-351
4) Hara T, Phuong PT, Fukuda D, Yamaguchi K, Murata C, Nishimoto S, Yagi S, Kusunose K, Yamada H, Soeki T, Wakatsuki T, Imoto I, Shimabukuro M, Sata M: Protease - Activated Receptor - 2 Plays a Critical Role in Vascular Inflammation and Atherosclerosis in Apolipoprotein E - Deficient Mice. Circulation, 2018; 138: 1706-1719
5) Ranjan S, Goihl A, Kohli S, Gadi I, Pierau M, Shahzad K, Gupta D, Bock F, Wang H, Shaikh H, Kähne T, Reinhold D, Bank U, Zenclussen AC, Niemz J, Schnöder TM, Brunner-Weinzierl M, Fischer T, Kalinski T, Schraven B, Luft T, Huehn J, Naumann M, Heidel FH, Isermann B: Activated protein C protects from GvHD via PAR2/PAR3 signalling in regulatory T-cells. Nat Commun, 2017; 8: 311
6) Antoniak S, Rojas M, Spring D, Bullard TA, Verrier ED, Blaxall BC, Mackman N, Pawlinski R: Protease-Activated Receptor 2 Deficiency Reduces Cardiac Ischemia/Reperfusion Injury. Arterioscler Thromb Vasc Biol, 2010; 30: 2136-2142
7) Borensztajn K, Peppelenbosch MP, Spek CA: Factor Xa: at the crossroads between coagulation and signaling in physiology and disease. Trends Mol Med, 2008; 14: 429-440
8) Kwapiszewska G, Markart P, Dahal BK, Kojonazarov B, Marsh LM, Schermuly RT, Taube C, Meinhardt A, Ghofrani HA, Steinhoff M, Seeger W, Preissner KT, Olschewski A, Weissmann N, Wygrecka M: PAR-2 inhibition reverses experimental pulmonary hypertension. Circ Res, 2012; 110: 1179-1191
9) Mega JL, Braunwald E, Wiviott SD, Bassand JP, Bhatt DL, Bode C, Burton P, Cohen M, Cook-Bruns N, Fox KA, Goto S, Murphy SA, Plotnikov AN, Schneider D, Sun X, Verheugt FW, Gibson CM; ATLAS ACS 2–TIMI 51 Investigators: Rivaroxaban in patients with a recent acute coronary syndrome. N Engl J Med, 2012; 366: 9-19
10) Hara T, Fukuda D, Tanaka K, Higashikuni Y, Hirata Y, Nishimoto S, Yagi S, Yamada H, Soeki T, Wakatsuki T, Shimabukuro M, Sata M: Rivaroxaban, a novel oral anticoagulant, attenuates atherosclerotic plaque progression and destabilization in ApoE-deficient mice. Atherosclerosis, 2015; 242: 639-646
11) Goto M, Miura S-I, Suematsu Y, Idemoto Y, Takata K, Imaizumi S, Uehara Y, Saku K: Rivaroxaban, a factor Xa inhibitor, induces the secondary prevention of cardiovascular events after myocardial ischemia reperfusion injury in mice. Int J Cardiol, 2016; 220: 602-607
12) Nakaoka H, Nakagawa-Toyama Y, Nishida M, Okada T, Kawase R, Yamashita T, Yuasa-Kawase M, Nakatani K, Masuda D, Ohama T, Sonobe T, Shirai M, Komuro I, Yamashita S: Establishment of a Novel Murine Model of Ischemic Cardiomyopathy with Multiple Diffuse Coronary Lesions. PLoS One, 2013; 8: e70755
13) Zhou Q, Bea F, Preusch M, Wang H, Isermann B, Shahzad K, Katus HA, Blessing E: Evaluation of plaque stability of advanced atherosclerotic lesions in apo E-deficient mice after treatment with the oral factor Xa inhibitor rivaroxaban. Mediators Inflamm, 2011; 2011: 432080
14) Zhou W, Zorn M, Nawroth P, Bütehorn U, Perzborn E, Heitmeier S, Veltkamp R: Hemostatic therapy in experimental intracerebral hemorrhage associated with rivaroxaban. Stroke, 2013; 44: 771-778
15) Iba T, Aihara K, Yamada A, Nagayama M, Tabe Y, Ohsaka A: Rivaroxaban attenuates leukocyte adhesion in the microvasculature and thrombus formation in an experimental mouse model of type 2 diabetes mellitus. Thromb Res, 2014; 133: 276-280
16) Sparkenbaugh EM, Chantrathammachart P, Mickelson J, van Ryn J, Hebbel RP, Monroe DM, Mackman N, Key

NS, Pawlinski R: Differential contribution of FXa and thrombin to vascular inflammation in a mouse model of sickle cell disease. Blood, 2014; 123: 1747-1756
17) Imano H, Kato R, Tanikawa S, Yoshimura F, Nomura A, Ijiri Y, Yamaguchi T, Izumi Y, Yoshiyama M, Hayashi T: Factor Xa inhibition by rivaroxaban attenuates cardiac remodeling due to intermittent hypoxia. J Pharmacol Sci, 2018; 137: 274-282
18) Getz GS, Reardon CA: Diet and murine atherosclerosis. Arterioscler Thromb Vasc Biol, 2006; 26: 242-249
19) Nishina PM, Verstuyft J, Paigen B: Synthetic low and high fat diets for the study of atherosclerosis in the mouse. J Lipid Res, 1990; 31: 859-869
20) Zhang S, Picard MH, Vasile E, Zhu Y, Raffai RL, Weisgraber KH, Krieger M: Diet-induced occlusive coronary atherosclerosis, myocardial infarction, cardiac dysfunction, and premature death in scavenger receptor class B type I-deficient, hypomorphic apolipoprotein ER61 mice. Circulation, 2005; 111: 3457-3464
21) Rigotti A, Trigatti BL, Penman M, Rayburn H, Herz J, Krieger M: A targeted mutation in the murine gene encoding the high density lipoprotein (HDL) receptor scavenger receptor class B type I reveals its key role in HDL metabolism. Proc Natl Acad Sci U S A, 1997; 94: 12610-12615
22) Raffa RL, Weisgraber KH: Hypomorphic apolipoprotein E mice: A new model of conditional gene repair to examine apolipoprotein E-mediated metabolism. J Biol Chem, 2002; 277: 11064-11068
23) Thum T, Gross C, Fiedler J, Fischer T, Kissler S, Bussen M, Galuppo P, Just S, Rottbauer W, Frantz S, Castoldi M, Soutschek J, Koteliansky V, Rosenwald A, Basson MA, Licht JD, Pena JT, Rouhanifard SH, Muckenthaler MU, Tuschl T, Martin GR, Bauersachs J, Engelhardt S: MicroRNA-21 contributes to myocardial disease by stimulating MAP kinase signalling in fibroblasts. Nature, 2008; 456: 980-984
24) Sengupta A, Molkentin JD, Paik JH, DePinho RA, Yutzey KE: FoxO transcription factors promote cardiomyocyte survival upon induction of oxidative stress. J Biol Chem, 2011; 286: 7468-7478
25) Oe Y, Hayashi S, Fushima T, Sato E, Kisu K, Sato H, Ito S, Takahashi N: Coagulation Factor Xa and Protease-Activated Receptor 2 as Novel Therapeutic Targets for Diabetic Nephropathy. Arterioscler Thromb Vasc Biol, 2016; 36: 1525-1533
26) Jones SM, Mann A, Conrad K, Saum K, Hall DE, McKinney LM, Robbins N, Thompson J, Peairs AD, Camerer E, Rayner KJ, Tranter M, Mackman N, Owens AP: PAR2 (Protease-Activated Receptor 2) Deficiency Attenuates Atherosclerosis in Mice. Arterioscler Thromb Vasc Biol, 2018; 38: 1271-1282
27) Asada Y, Yamashita A, Sato Y, Hatakeyama K: Thrombus Formation and Propagation in the Onset of Cardiovascular Events. J Atheroscler Thromb, 2018; 25: 653-664
28) McLarty JL, Meléndez GC, Brower GL, Janicki JS, Levick SP: Tryptase/Protease-activated receptor 2 interactions induce selective mapk signaling and collagen synthesis by cardiac fibroblasts. Hypertension, 2011; 58: 264-270
29) Borensztajn K, Stiekema J, Nijmeijer S, Reitsma PH, Peppelenbosch MP, Spek CA: Factor Xa stimulates proinflammatory and profibrotic responses in fibroblasts via protease-activated receptor-2 activation. Am J Pathol, 2008; 172: 309-320
30) Le T-TT, Karmouty-Quintana H, Melicoff E, Le TT, Weng T, Chen NY, Pedroza M, Zhou Y, Davies J, Philip K, Molina J, Luo F, George AT, Garcia-Morales LJ, Bunge RR, Bruckner BA, Loebe M, Seethamraju H, Agarwal SK, Blackburn MR: Blockade of IL-6 Trans Signaling Attenuates Pulmonary Fibrosis. J Immunol, 2014; 193: 3755-3768
31) Kayano K, Okita K: Does IL-6 regulate liver fibrosis / cirrhosis directly and indirectly? J Gastroenterol, 2000; 35: 250-251
32) Luckett-Chastain LR, Gallucci RM: Interleukin (IL)-6 modulates transforming growth factor-b expression in skin and dermal fibroblasts from IL-6-deficient mice. Br J Dermatol, 2009; 161: 237-248
33) Park GH, Jeon SJ, Ryu JR, Choi MS, Han SH, Yang SI, Ryu JH, Cheong JH, Shin CY, Ko KH: Essential role of mitogen-activated protein kinase pathways in protease activated receptor 2-mediated nitric-oxide production from rat primary astrocytes. Nitric Oxide, 2009; 21: 110-119
34) Lim SY, Tennant GM, Kennedy S, Wainwright CL, Kane KA: Activation of mouse protease-activated receptor-2 induces lymphocyte adhesion and generation of reactive oxygen species. Br J Pharmacol, 2006; 149: 591-599
35) Patel MR, Mahaffey KW, Garg J, Pan G, Singer DE, Hacke W, Breithardt G, Halperin JL, Hankey GJ, Piccini JP, Becker RC, Nessel CC, Paolini JF, Berkowitz SD, Fox KA, Califf RM; ROCKET AF Investigators: Rivaroxaban versus Warfarin in Nonvalvular Atrial Fibrillation. N Engl J Med, 2011; 365: 883-891
36) EINSTEIN–PE Investigators, Büller HR, Prins MH, Lensin AW, Decousus H, Jacobson BF, Minar E, Chlumsky J, Verhamme P, Wells P, Agnelli G, Cohen A, Berkowitz SD, Bounameaux H, Davidson BL, Misselwitz F, Gallus AS, Raskob GE, Schellong S, Segers A: Oral rivaroxaban for the treatment of symptomatic pulmonary embolism. N Engl J Med, 2012; 366: 1287-1297
37) EINSTEIN Investigators, Bauersachs R, Berkowitz SD, Brenner B, Buller HR, Decousus H, Gallus AS, Lensing AW, Misselwitz F, Prins MH, Raskob GE, Segers A, Verhamme P, Wells P, Agnelli G, Bounameaux H, Cohen A, Davidson BL, Piovella F, Schellong S: Oral rivaroxaban for symptomatic venous thromboembolism. N Engl J Med, 2010; 363: 2499-2510
38) Connolly SJ, Eikelboom JW, Bosch J, Dagenais G, Dyal L, Lanas F, Metsarinne K, O'Donnell M, Dans AL, Ha JW, Parkhomenko AN, Avezum AA, Lonn E, Lisheng L, Torp-Pedersen C, Widimsky P, Maggioni AP, Felix C, Keltai K, Hori M, Yusoff K, Guzik TJ, Bhatt DL, Branch KRH, Cook Bruns N, Berkowitz SD, Anand SS, Varigos JD, Fox KAA, Yusuf S; COMPASS investigators: Rivaroxaban with or without aspirin in patients with stable coronary artery disease: An international, randomised, double-blind, placebo-controlled trial. The Lancet, 2018; 391; 205-218
39) Nakamura M, Yamada N, Ito M: Direct Oral Anticoagulants for the Treatment of Venous Thromboembolism in Japan. J Atheroscler Thromb, 2017; 24: 560-565

40) Zannad F, Anker SD, Byra WM, Cleland JGF, Fu M, Gheorghiade M, Lam CSP, Mehra MR, Neaton JD, Nessel CC, Spiro TE, van Veldhuisen DJ, Greenberg B; COMMANDER HF Investigators: Rivaroxaban in Patients with Heart Failure, Sinus Rhythm, and Coronary Disease. N Engl J Med, 2018; 379: 1332-1342

41) Piccoli MT, Gupta SK, Viereck J, Foinquinos A, Samolovac S, Kramer FL, Garg A, Remke J, Zimmer K, Batkai S, Thum T: Inhibition of the Cardiac Fibroblast-Enriched lncRNA Meg3 Prevents Cardiac Fibrosis and Diastolic Dysfunction. Circ Res, 2017; 121: 575-583

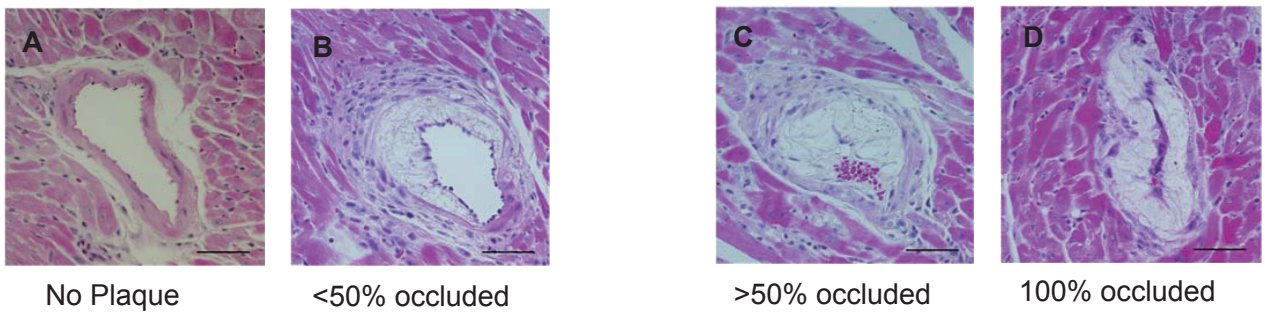

Supplemental Fig. 1. Evaluation of occluded coronary arteries

Representative images of various extents of occluded coronary arteries (A, no plaque; B, <50% occluded; C, >50% occluded; D, 100% occluded). Bar=50 μm.

Supplemental Table 1. Mouse Primer sequence

	Forward primer	Reverse primer
Nppa	5'-GCTTCCAGGCCATATTGGAG-3'	5'-GGGGGCATGACCTCATCTT-3'
Nppb	5'-GAGGTCACTCCTATCCTCTGG -3'	5'-GCCATTTCCTCCGACTTTTCTC -3'
IL-1β	5'-TGAAGTTGACGGACCCCAAA-3'	5'-TGATGTGCTGCTGCGAGATT-3'
IL-6	5'-ACAACCACGGCCTTCCCTACTT-3'	5'-CACGATTTCCCAGAGAACATGTG-3'
NF-κB	5'-TACAAGCTGGCTGGTGGGGA-3'	5'-GTCGCGGGTCTCAGGACCTT-3'
TNF-α	5'-TGTGCTCAGAGCTTTCAACAAC-3'	5'-GCCCATTTGAGTCCTTGATG-3'
MMP-9	5'-CATTCGCGTGGATAAGGAGT-3'	5'-ACCTGGTTCACCTCATGGTC-3'
MMP-12	5'-TACCCCAAGCTGATTTCCACAC-3'	5'-CTCCTTGGAAGATGTAGTAGTGTCTTT-3'
TIMP1	5'-CGGCCCGTGATGAGAAACT-3'	5'-GCAACTCGGACCTGGTCATAA-3'
TGFβ 1	5'-CACAGATCTGATGGATTTCAAGA-3'	5'-CCTCATCTTCTACCGGCATC-3'
COL-1	5'-AGCCTCGCTCCCAGCCTTCA -3'	5'-CCTGGGCGCGGCTGTATGAG-3'
COL-3	5'-CCCTGGACCTCAGGGTATCA-3'	5'-GGGTTTCCATCCCTTCCAGG-3'
PAR1	5'-GTCTTCCCGCGTCCCTAT-3'	5'-GGGTTCACCGTAGCATCTGT-3'
PAR2	5'-GGACCGAGAACCTTGCAC-3'	5'-GGAACCCCTTTCCCAGTG-3'
GAPDH	5'-ACTCCACTCACGGCAAATTC-3'	5'-TCTCCATGGTGGTGAAGACA-3'

Supplemental Table 2. Rat Primer sequence

	Forward primer	Reverse primer
IL-1β	5'-TGTGATGAAAGACGGCACAC-3'	5'-CTTCTTCTTTGGGTATTGTTTGG-3'
IL-6	5'-CCCTTCAGGAACAGCTATGAA-3'	5'- ACAACATCAGTCCCAAGAAGG-3'
TNF-α	5'-TGAACTTCGGGGTGATCG-3'	5'-GGGCTTGTCACTCGAGTTTT-3'
MMP-9	5'-CCTCTGCATGAAGACGACATAA-3'	5'-GGTCAGGTTTAGAGCCACGA-3'
COL-1	5'-TCCTGGCAAGAACGGAGAT-3'	5'-CAGGAGGTCCACGCTCAC-3'
PAR1	5'-CGGTCCTTTGCTGTCTTCC-3'	5'-ACGGCGTAGCATACATCCTC-3'
PAR2	5'-GGCTGCTGGGAGGTATCAC-3'	5'-CGTGTCCAATCTGCCAATC-3'
β-actin	5'-CGTCATCCATGGCCAACT-3'	5'-CCCGCGAGTACAACCTTCT-3'